# Creating different polarisations using sub wavelength slits in a zigzag pattern

M. Bogers

July 2012

**Abstract**

I have studied a nanodevice to find out if it can separate left- and right-handed circularly polarised light in the far field. The device used was a subwavelength zigzag grating, illuminated with linearly polarised light. The light transmitted through the zigzag was measured in the near and the far field regime.
In the near field the light is elliptically polarised. The grating, under 633 nm light, functions like a quarter-wave retarder; in a zigzag with an internal angle of 90°, the 'zigs' emit left- and the 'zags' emit right-handed circularly polarised light.
In the far field, left- and right-handed circularly polarised light are separated along the diagonals of the diffraction pattern, for a 90° zigzag illuminated by 633 nm light. Between two such diagonals the light takes on intermediate states of polarisation.

# 1 Introduction

Around the middle of the previous century the integrated circuit enabled the miniaturisation of electronic equipment. Within photonics a similar endeavour is being made to create integrated optics. Integrated optics will reduce the size of optical elements so light can be created and manipulated on a single chip; this should enable optical computation. One of the tools that will be used in this enterprise will be metallic structures on a nanoscale. An interesting example of these structures are metallic waveguides, which function as active nanodevices, that have surprising properties on a subwavelength scale.

In a perfectly conducting planar waveguide there can be no electric field parallel to the surface. When an electromagnetic wave, with wavelength $\lambda$, passes through the waveguide, only normal modes that have no parallel electric component at the surface can be sustained. The narrowest waveguide at which such a mode might exist is $\lambda/2$ wide. Narrower waveguides will therefore only transmit light that has an electric field perpendicular to the slit; they work as a linear polariser.

Interestingly, contrary to the predictions of the simple model, transmission occurs in narrower slits and does not have a definite cutoff width. Additionally the parallel and the perpendicular components of the wave incur a relative phase difference during transmission. These discrepancies are due to metals not being perfect conductors and there are several effects that need to be taken into account[1]:

- Parallel electric fields can permeate the metal, although how deeply depends on the wavelength; as a result the cutoff width is smaller than $\lambda/2$ and the parallel and perpendicular modes propagate at different speeds.
- The wave component perpendicular to the slit excites surface plasmons, which are waves in the electron sea of the metal surface, and loses energy.

In experiment [1] it was shown that slits, at a certain width narrower than $\lambda/2$, have equal perpendicular and parallel electric field amplitude transmission, and that for the right width a slit can function as a quarter-wave retarder. It has been proposed that, alternatively, an array of crosses with asymmetrical arms may also function as a quarter-wave retarder [2]. Some use of these retarders could be to shape and delay ultra-short pulses [3].

This experiment is an expansion of experiment [1]. In this experiment I study the diffraction from a zigzag array of slits (see Figure 1). Each slit should behave like a distinct quarter-wave plate with its fast axis parallel to the long dimension of the slit. The research question is: when illuminating the zigzag grating with linearly polarised light, can the left- and right-handed circular polarisation in the far field regime of the grating be separated? This could be an interesting way to create different types of polarisation.

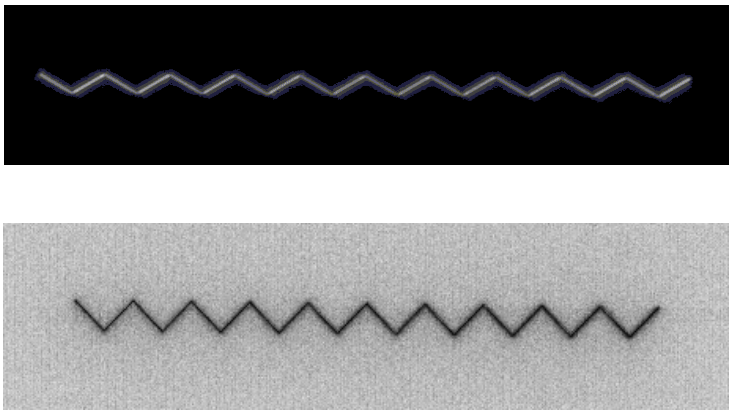


Figure 1: Images of the zigzags. The segments are at 90° and 120° internal angles, each segment has a length of 10 $\mu$m and a width of 200 nm. The picture of the 120° zigzag was made by an optical microscope, and the picture of the 90° zigzag was made by a scanning electron microscope.

In the experiment it was demonstrated that a zigzag grating can separate different polarisations along diagonal directions. For the correct wavelength, these slits can function as a quarter-wave plate. In that case, the light on a diagonal line in the far field, perpendicular to the long side of the slit, has the same polarisation as the slit in the far field. In between those diagonals, the far-field light has intermediate states of polarisation (see Figure 21).

## 2 Theory

In this section I will calculate the far field diffraction pattern from the subwavelength zigzag grating. I will work through the constituent elements of the zigzag to understand their function. These elements will then be assembled to predict the zigzag's far field diffraction pattern. First I will regard the light transmitted through one slit. Then I shall consider the far field diffraction pattern of the light from this slit. Lastly, I will give the diffraction pattern of the whole zigzag.

**Transmission of a slit.**

The transmission of the slit has been treated (see ref. [1]), this is a summary of that exposition.

To predict the transmission of light through the slit, I model it as follows: the laser beam is monochromatic, vertically polarized and approximates a plane wave at the scale of the slits. This beam impinges perpendicularly on the gold film.

The gold film does not transmit light and has a permittivity $\epsilon$ dependent on the wavelength. On the gold film there are slits, these are rectangular and have a far greater length than width. Each slit is modelled as infinitely long so it simplifies to a planar waveguide in the analysis.

The waveguide's width is limited so only the fundamental mode doesn't evanesce. There are then two modes in the wave guide: a transverse electric (TE) and a transverse magnetic (TM) mode.

The gold layer has a finite conductivity; this is modelled by a waveguide surface that is not an ideal conductor and so the medium in the waveguide has a complex propagation constant $\beta_i = \frac{n_i^{\text{eff}}}{k_0}$, where $i$ = TM or $i$ = TE.

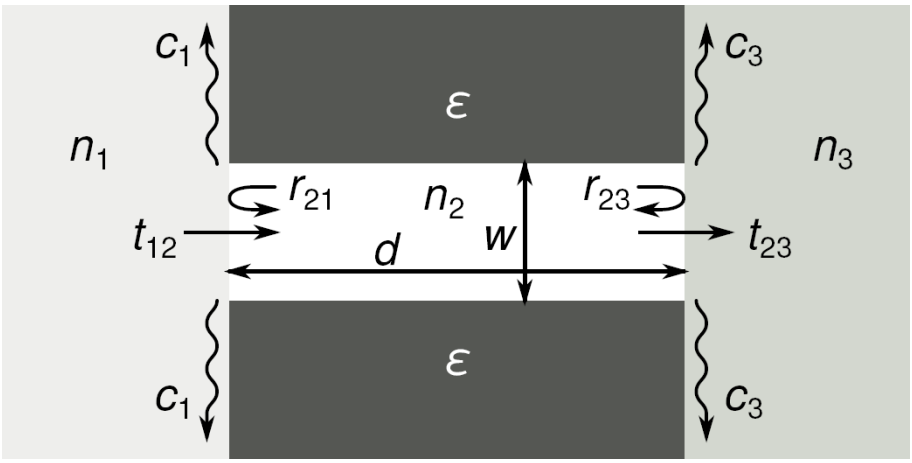


Figure 2: A cross section of the planar waveguide, with the relevant quantities indicated [1]

Now the functioning of the wave guide will be regarded (See Figure 2). From the air, with index $n_1$, there is a plane wave incident on the slit. This is coupled into the waveguide, with index $n_2$, which in this model we assume equal to $n^{\text{eff}}$. Inside the waveguide there is reflection and transmission at the interfaces. A part transmits into the glass, which has index $n_3$. The associated complex amplitude reflection and transmission coefficients $r_{12}, r_{23}, t_{12}$ and $t_{23}$ are shown in the figure.
Using the refractive indices of the media, the Fresnel conditions give the proportions of the refracted and reflected light and give the phase shift of the latter. The internal reflections in the wave guide make it a resonator, specifically a Fabry-Pérot etalon. The formula for the complex amplitude transmission through the an etalon of thickness $d$ is

$$t_{123} = t_{12}t_{23}\frac{e^{i\beta d}}{1 - r_{12}r_{23}e^{i2\beta d}} \tag{1}$$

The TM mode in the resonator couples to the plasmons on the surface of the gold layer. This causes surface plasmon polaritons to be launched on the surface around the slit, which decrease the intensity transmitted for the TM mode. The constants that represent the amount of coupling at the interfaces are $c_1$ and $c_3$. Using the complex amplitude transmission and the intensity of the plasmons, the intensity transmission coefficients and phase difference between the two modes can be calculated (see ref. [1]).

$$\begin{aligned} T_{\text{TE}} &= \frac{n_3}{n_1}|t_{123}^{\text{TE}}|^2 \\ T_{\text{TM}} &= \frac{n_3}{n_1}|t_{123}^{\text{TM}}|^2 - 2|c_1|^2 - 2|c_3|^2 \\ \Delta\phi &= \arg t_{123}^{\text{TM}} - \arg t_{123}^{\text{TE}} \qquad mod(2\pi) \end{aligned} \tag{2}$$

This describes the light transmitted from the waveguide dependent on its width. The phase relation has been tested and is found to agree with experiment (figure 4b, ref. [1]) My experiment has been designed such that, barring manufacturing or material discrepancies, each slit should behave as a quarter-wave plate. In this analogy the fast axis of the quarter-wave plate is parallel to the slit. In the following I will assume that these properties are consistent for all slits.

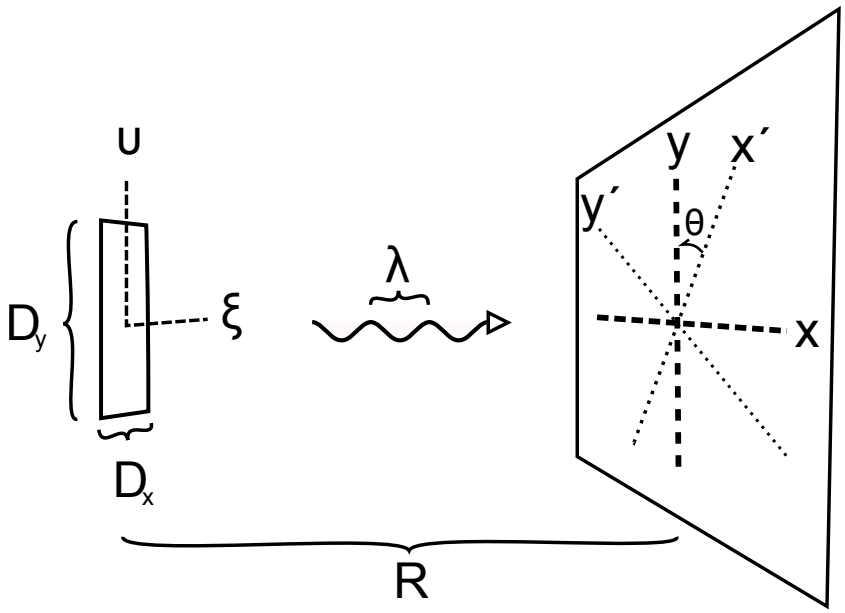


Figure 3: An image of the relevant quantities in diffraction from a single slit

**The diffraction of the slit**

In the following I will determine the electric field of the far-field diffraction of light from a slit. First I will investigate the far-field diffraction of the light from one slit (see Figure 3). I will assume that each slit is a rectangle and radiates polarised light uniformly from each point of the aperture, so initially I will omit the polarisation. I will then rotate the diffraction patterns of a slit, because in a zigzag the slit is oriented at an angle $\theta$ with respect to the horizontal. Finally, I will give an expression for the polarisation of the light that emerges from the slits.

The Huygens-Fresnel principle states that each point on a wave-front induces a spherical wave. The summation of these secondary waves determines later wave fronts. When spherical waves expand a great distance, or pass through a convergent lens, they approach being plane waves. A projection of these plane waves results in an irradiance that only depends on their phase differences, which result from different optical paths. Where this approximation holds, one speaks of Fraunhofer diffraction.
In the Fraunhofer approximation the complex representation of the wave is

$$\Psi(x, y, \xi, \upsilon, t) = \frac{E_0}{R} e^{i(kR-\omega t)} e^{-ik\frac{(x\xi+y\upsilon)}{R}}$$

Integrating this over the area of the slit gives the electric field of the Fraunhofer diffraction pattern

$$\Psi_{\text{slit}}(x, y, t) = \frac{E_0}{R} e^{i(kR-\omega t)} D_x D_y \operatorname{sinc}\left(\frac{\pi D_x x}{\lambda R}\right) \operatorname{sinc}\left(\frac{\pi D_y y}{\lambda R}\right)$$

On the zigzag the slits are oriented at an angle $\theta$ to the horizontal axis $x'$. This correction is made by applying a rotation to the coordinates (see Figure 3). This rotation is described by the following matrix multiplication:

$$\begin{pmatrix} x \\ y \end{pmatrix} = \begin{pmatrix} \sin\theta & -\cos\theta \\ \cos\theta & \sin\theta \end{pmatrix} \begin{pmatrix} x' \\ y' \end{pmatrix}.$$

In the notation I will indicate this rotation of the coordinates in the complex amplitude of the slit by $\hat{R}(\theta)$. I will then write complex amplitude of the 'zag' slit as

$$\Psi_{\diagup} = \hat{R}(\theta)\Psi_{\text{slit}}$$

and the complex amplitude of the 'zig' slit as

$$\Psi_{\diagdown} = \hat{R}(-\theta)\Psi_{\text{slit}}$$

Each slit is illuminated by vertically polarised light and functions as a quarter-wave plate, where the long side of the slit is the fast axis. One can introduce a uniform polarization of light by multiplying by a complex vector [4]. The polarised light emitted by a slit, at an angle $\theta$, then has the following complex polarisation vector:

$$\hat{e}(\theta) = \frac{1}{\sqrt{2}} (\sin(2\theta), \cos(2\theta) + i)$$

**The diffraction of the zigzag**

Finally these elements can be combined to find the Fraunhofer diffraction pattern of the polarized light from the zigzag lattice. It will be assumed that, apart from rotations and translations, the slits are identical. Furthermore there is no interaction between the slits, even where they overlap (i.e. the angles).
Mathematically the Fraunhofer diffraction pattern is the Fourier transform of the aperture function. The convolution theorem states that the Fourier transform of an array of identical apertures equals the Fourier transform of one aperture times the Fourier transform of the centres of the apertures, which are indicated by $\delta$-functions. The zigzag pattern is the sum of two convolutions (see Figure 4).

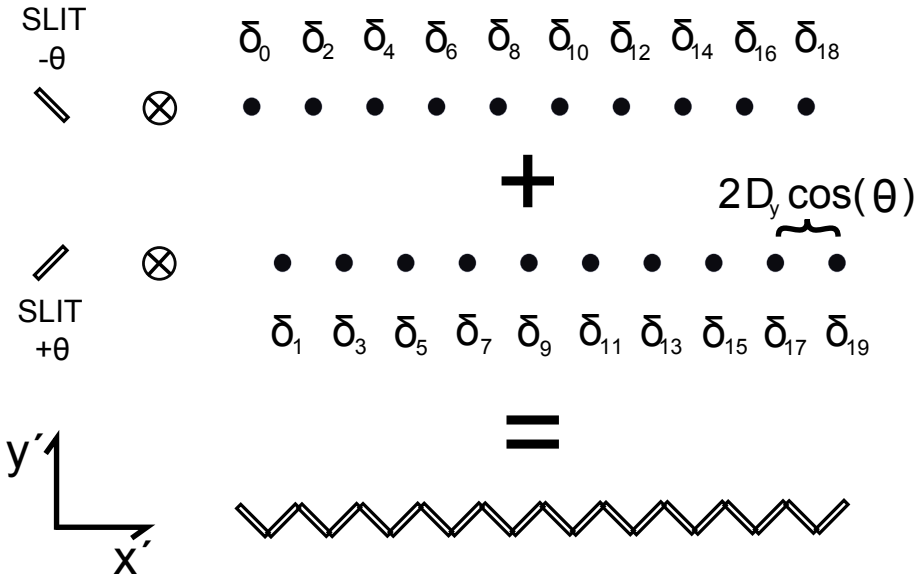


Figure 4: A view of two convolutions. The convolution of a 'zig' and a train of $\delta$-functions creates the row of zigs in the zigzag. The convolution of a 'zag' and a train of $\delta$-functions creates the row of zags in the zigzag. The summation of these convolutions gives the zigzag pattern.

The Fourier transform of the slit has been treated. The zigzag consists of $N$ (=10) zigs and $N$ zags, and is placed symmetrically around the $y'$-axis. The row of zags is represented by a train of $\delta$-functions in the convolution. The Fourier transform this train of $\delta$-functions is

$$T_{\diagup} = \mathrm{sinc}(N\phi)e^{i\frac{\phi}{2}} \qquad \text{where } \phi = \frac{kx'D_y\cos(\theta)}{R}$$

Similarly, the Fourier transform of the train of $\delta$-functions representing the row of zigs is

$$T_{\diagdown} = \mathrm{sinc}(N\phi)e^{-i\frac{\phi}{2}}$$

A simple assembly of the parts, now gives the complex amplitude of the zigzag is

$$\begin{aligned} \overrightarrow{\Psi}_{\text{zigzag}} &= \left(T_{\diagup}\hat{e}(\theta)\hat{R}(\theta) + T_{\diagdown}\hat{e}(-\theta)\hat{R}(-\theta)\right)\Psi_{\text{slit}} \\ &= \left(T_{\diagup}\hat{e}(\theta)\Psi_{\diagup} + T_{\diagdown}\hat{e}(-\theta)\Psi_{\diagdown}\right) \end{aligned} \tag{3}$$

It is useful to characterize the diffraction in terms of observable traits, so I calculate the Stokes parameters. These are defined as follows:

- $S_0$ is the total intensity; it is the sum of the horizontal and vertical linearly polarised component of the intensity.

$$\begin{aligned} S_0 &= |\overrightarrow{\Psi}_{\text{zigzag}} \cdot \hat{x}|^2 + |\overrightarrow{\Psi}_{\text{zigzag}} \cdot \hat{y}|^2 \\ &= \operatorname{sinc}^2(N\phi)(\Psi_{\diagup}^2 + \Psi_{\diagdown}^2 + 2\cos(\phi)\cos^2(2\theta)\Psi_{\diagup}\Psi_{\diagdown}) \end{aligned} \tag{4}$$

- $S_1$ is the difference between the horizontal and vertical linearly polarised component of the intensity.

$$\begin{aligned} S_1 &= |\overrightarrow{\Psi}_{\text{zigzag}} \cdot \hat{x}|^2 - |\overrightarrow{\Psi}_{\text{zigzag}} \cdot \hat{y}|^2 \\ &= -\operatorname{sinc}^2(N\phi)\left((\Psi_{\diagup}^2 + \Psi_{\diagdown}^2)\cos^2(2\theta) + 2\cos(\phi)\Psi_{\diagup}\Psi_{\diagdown}\right) \end{aligned} \tag{5}$$

- $S_2$ is the difference between the diagonal and anti-diagonal linearly polarised component of the intensity;

$$\begin{aligned} S_2 &= |\overrightarrow{\Psi}_{\text{zigzag}} \cdot \frac{\hat{x}+\hat{y}}{\sqrt{2}}|^2 - |\overrightarrow{\Psi}_{\text{zigzag}} \cdot \frac{\hat{x}-\hat{y}}{\sqrt{2}}|^2 \\ &= \operatorname{sinc}^2(N\phi)\sin(2\theta)\left((\Psi_{\diagup}^2 - \Psi_{\diagdown}^2)\cos(2\theta) + 2\sin(\phi)\Psi_{\diagup}\Psi_{\diagdown}\right) \end{aligned} \tag{6}$$

- $S_3$ is the difference between the right and left circularly polarised component of the intensity.

$$\begin{aligned} S_3 &= |\overrightarrow{\Psi}_{\text{zigzag}} \cdot \frac{\hat{x}-i\hat{y}}{\sqrt{2}}|^2 - |\overrightarrow{\Psi}_{\text{zigzag}} \cdot \frac{\hat{x}+i\hat{y}}{\sqrt{2}}|^2 \\ &= \operatorname{sinc}^2(N\phi)\sin(2\theta)\left(\Psi_{\diagup}^2 - \Psi_{\diagdown}^2 - 2\sin(\phi)\cos(2\theta)\Psi_{\diagup}\Psi_{\diagdown}\right) \end{aligned} \tag{7}$$

A convenient representation of the relative intensities is the set of normalised Stokes parameters: $s_1 = S_1/S_0$, $s_2 = S_2/S_0$, $s_3 = S_3/S_0$. These I will use to model the outcome of the measurements.

**Simulation**

I have used MATLAB to plot the intensity and the normalised Stokes parameters of the diffraction pattern that resulted from the calculation. These are plotted in Figures 6 and 7. The normalised Stokes parameters are shown in a blue and orange colour scale that represents a range between -1 and +1. In this colour scale the orange has a positive value, whereas the blue has a negative one. The signs indicate the nature of the polarisation components (see Figure 5).

- If $s_1$ is positive then the polarisation has a horizontal component, if negative, then it is vertical.
- If $s_2$ is positive then the polarisation has a diagonal (45° counterclockwise) component, if negative, then it is anti-diagonal (45° clockwise).
- If $s_3$ is positive then the polarisation has a right-handed component, if negative, then it is left-handed.

The relative colour saturations between the Stokes parameters indicates their contribution to the total polarisation.

To make the structure of the far-field diffraction pattern more clearly visible, I have also plotted the logarithm of $S_0$ for both zigzag gratings in Figure 8.

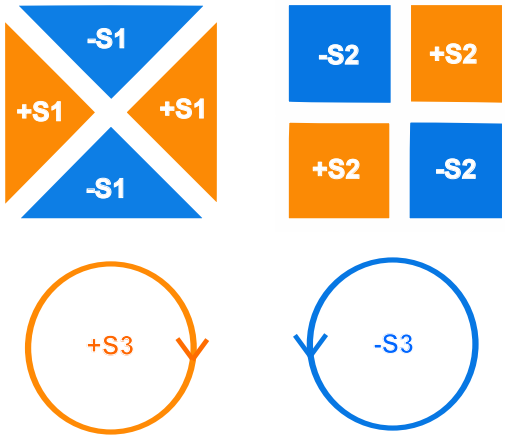


Figure 5: The distribution of the components of the normalised Stokes parameters. $s_1$ represents the difference between the horizontal and vertical intensity components. $s_2$ represents the difference between the diagonal and anti-diagonal intensity components. $s_3$ represents the difference between the right handed and left handed circular intensity components.

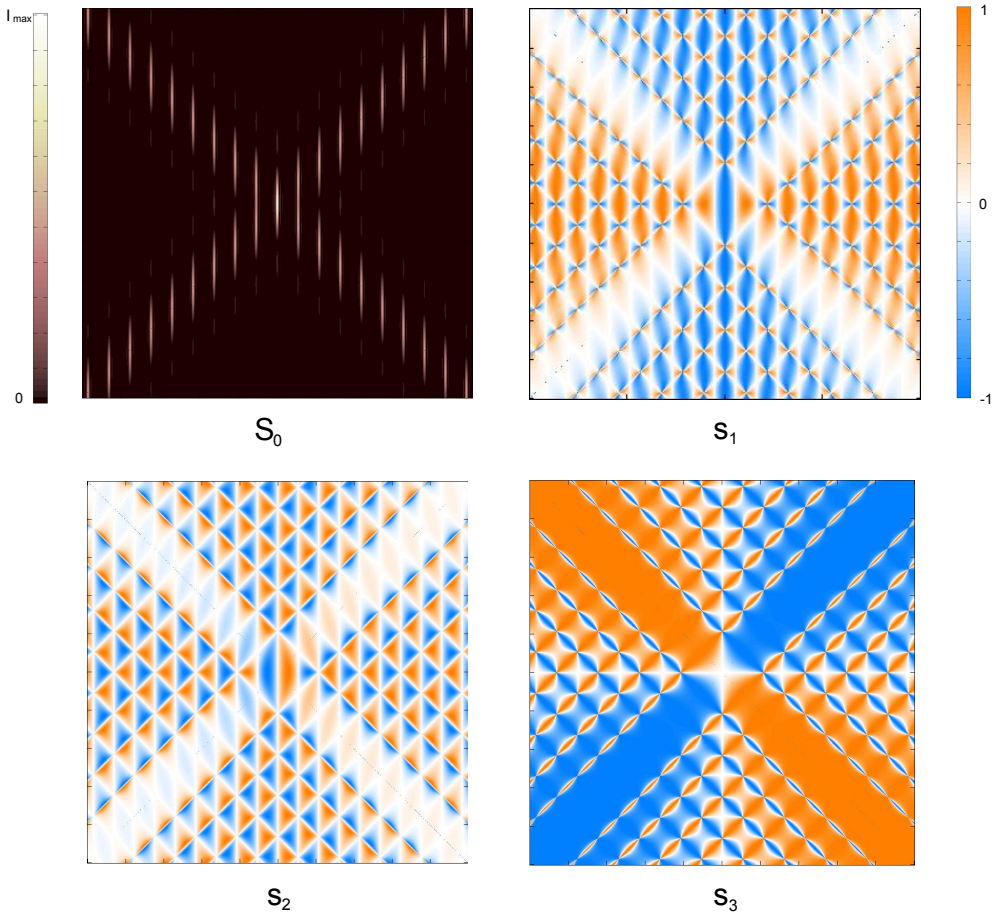


Figure 6: Theoretical far field diffraction of the 90° zigzag. If $s_1$ is positive then the polarisation has a horizontal component; if negative, then it is vertical. If $s_2$ is positive then the polarisation has a diagonal component; if negative, then it is anti-diagonal. If $s_3$ is positive then the polarisation has a right-handed component; if negative, then it is left-handed. The relative saturations indicate their contribution to the total polarisation.

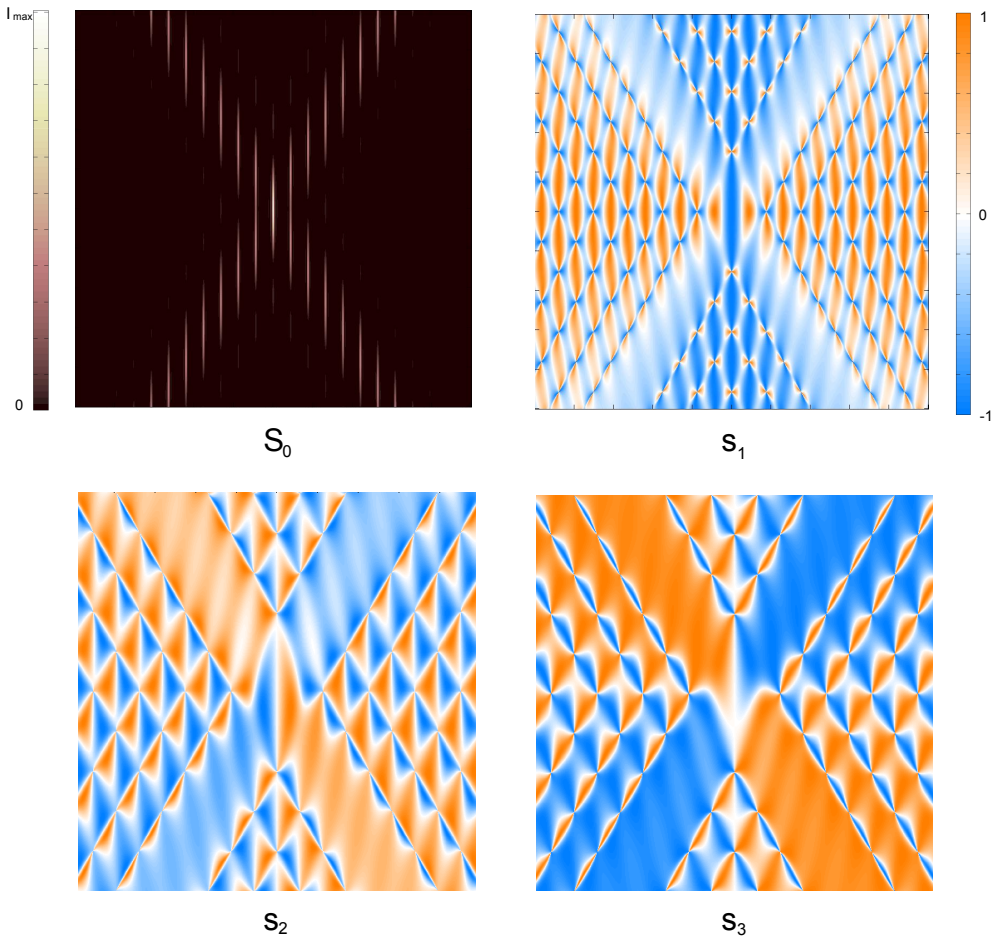


Figure 7: Theoretical far field diffraction of the 120° zigzag. If $s_1$ is positive then the polarisation has a horizontal component; if negative, then it is vertical. If $s_2$ is positive then the polarisation has a diagonal component; if negative, then it is anti-diagonal. If $s_3$ is positive then the polarisation has a right-handed component; if negative, then it is left-handed. The relative saturations indicate their contribution to the total polarisation.

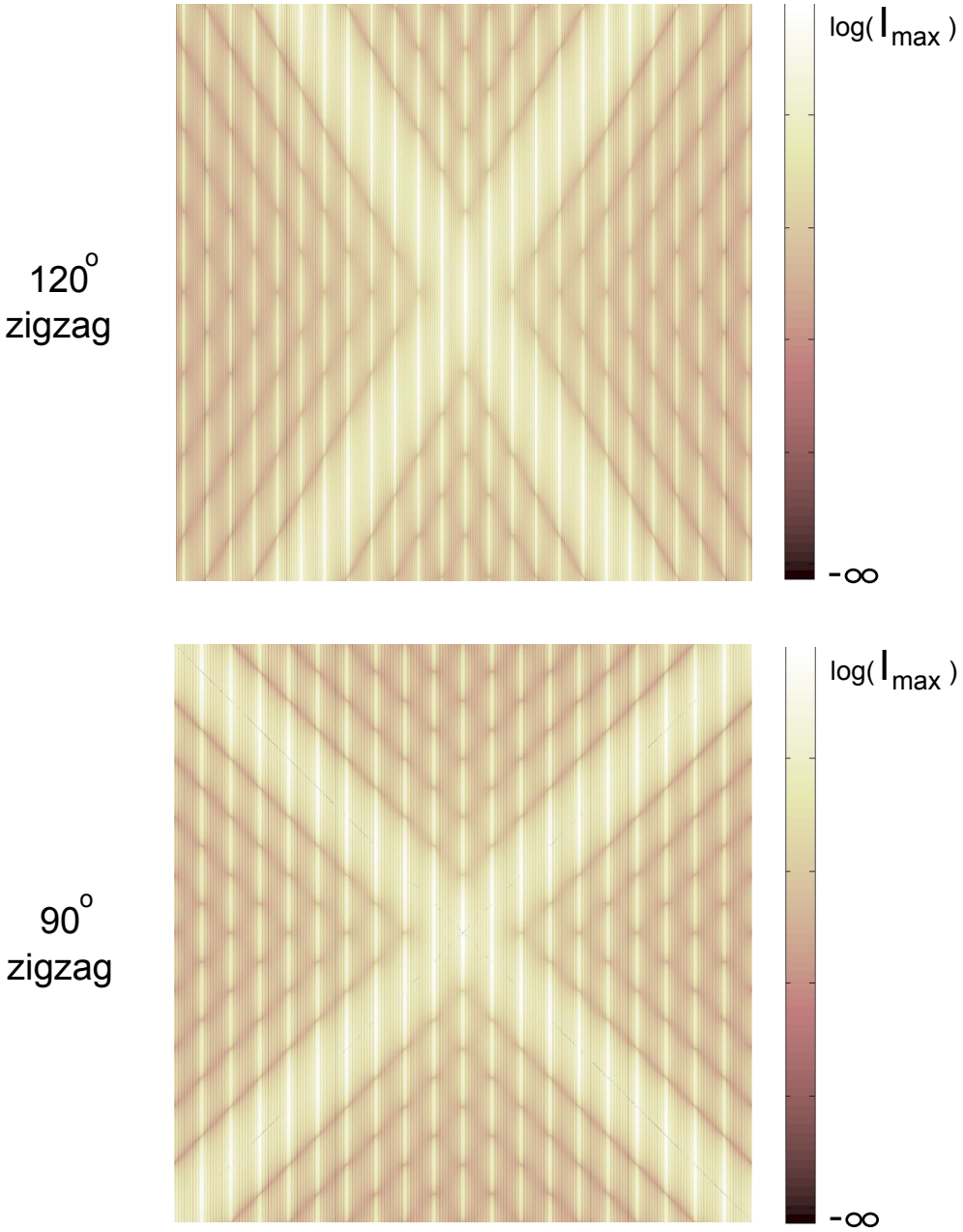


Figure 8: Logarithmic plots of the intensities of the diffraction patterns of the 90° and 120° zigzags, which show the structures of the diffraction patterns more clearly.

The general features of the simulation can be understood as follows:
The far-field diffraction from a single slit, of width $D$, is proportional to $\mathrm{sinc}(\frac{\pi D x}{\lambda R})$. The angular spread of the single slit diffraction is therefore inversely proportional to the width of the slit. There will thus be very little spread of the electric field parallel to the slit, but a wide spread perpendicular to the slit. These directions are independent, so the complex amplitude of the entire rectangular slit is proportional to the product of the perpendicular and parallel amplitude (see Figure 9). In the figures the relation between the shape of the slit and the shape of the diffraction pattern is clear. Naturally the diffraction has the same polarisation as the slit. The slit functions as a quarter-wave plate, and so the polarisation and shape of the diffraction pattern are dependent on the orientation of the slit.
The complex amplitude of the diffraction pattern of a zigzag is the summation of the amplitudes of the individual zigs and zags. Because the slits have a periodic spacing, each of their complex amplitudes incurs a multiple of a phase difference. There is positive interference on the camera only in positions where the phases of the all the individual slits are equal. This means that the diffraction pattern from a zigzag has a periodic positive interference, which manifests as bright vertical fringes.

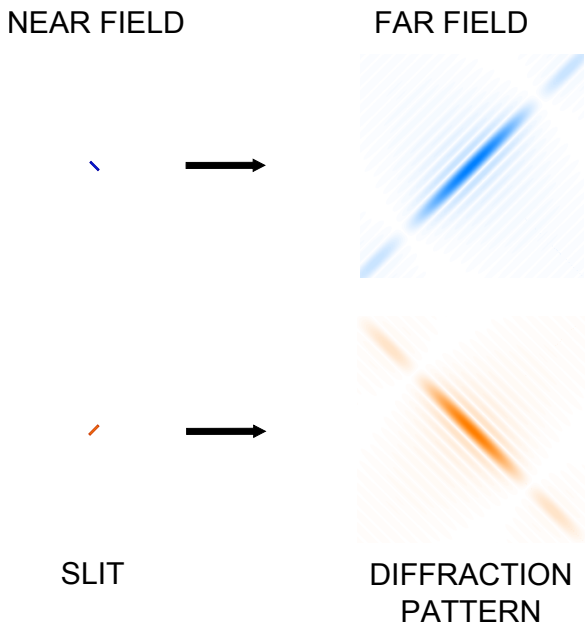


Figure 9: An image of the simple diffraction from one slit.

Between the diagonals, which are already sufficiently explained, there is a more complex structure. I will regard the plot of the normalised Stokes parameters of the 90° grating, in the upper and lower quadrant. A similar analysis, however, applies to the side quadrants.
In the $s_1$ and $s_2$ plot, there is a pattern of rhombi which is demarcated by white lines. These lines indicate there is only circularly polarised light there, as seen in $s_3$. This occurs when the right circularly polarised complex amplitude is zero, where the left circularly polarised complex amplitude is not; and vice versa. Therefore these rhombi occur in the overlay of the higher orders of the sinc-functions. I will use these rhombi as building blocks to explain the larger structures.
The colour saturation of the rhombi in $s_1$ and $s_2$ is dependent on the superposition of the different circular polarisations. The overlapping opposite circular polarisation creates the amount of linear polarisation, the excessive circular polarisation determines the value of $s_3$. This implies that the circularity of the polarisation depends on the difference in order of the overlapping zig and zag complex amplitude; the polarisation is therefore linear between two diagonals of the diffraction pattern.
The circular polarisation is created from vertical polarisation by a quarter-wave plate, so the vertical components are still in phase. When they superimpose where all incident light is in phase, indicated by the bright fringes in $S_0$, a vertical linear polarisation is regained. This can be seen as a vertical white line in the centre of a rhombus in $s_2$, and a blue colour in that position in $s_1$.
Moving horizontally, away from the central white $s_2$ line, the phase of one circular polarisation increases while the phase of the other decreases. This leads to a rotation of the linear polarisation (see Figure 10). This is clearly characterised by the following facts:
The diagonal polarisation changes sign around the central white line.
At distances, intermediate between the white $s_2$ line and the corners of the rhombus, there are white lines in $s_1$; here the polarisations are diagonal and antidiagonal.
From these blocks the figures of $s_1$ and $s_2$ can be constructed (see Figure 11).

In the analysis of the 120° grating, the structure is roughly the same. In this case however, the symmetry is degenerated. The diagonals of the diffraction pattern are at a different angle and the zigzag transmits elliptically polarised light. This means that there is a direct contribution to $s_1$ and $s_2$ by the light from the slit, which deforms the distribution of the polarisations in the rhombi.

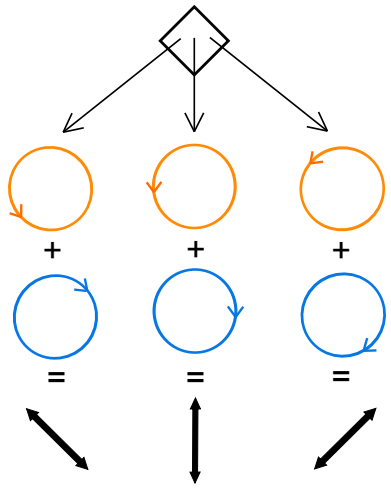

Figure 10: image of how the circular polarisations add up to create linear polarisations along the horizontal direction of the patterns.

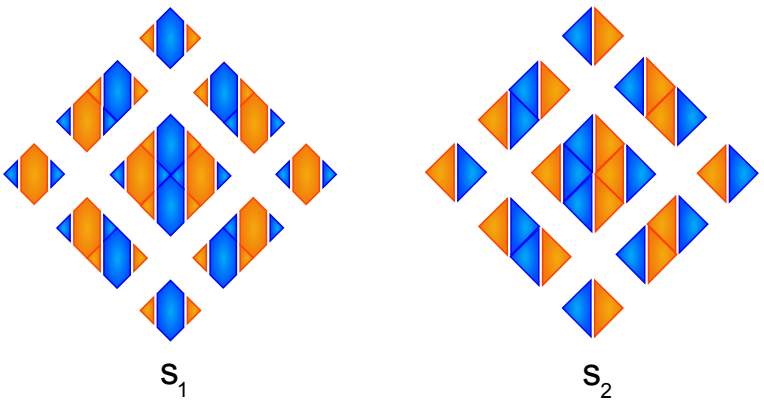


Figure 11: Image of how the rhombi from the different quadrants combine to create the diagonals and the centre of the $s_1$ and $s_2$ patterns. The corners of the figures are the rhombi, the sides of the figure are the diagonals of the diffraction pattern and the centre of the figure is the centre of the diffraction pattern.

# 3 Experimental

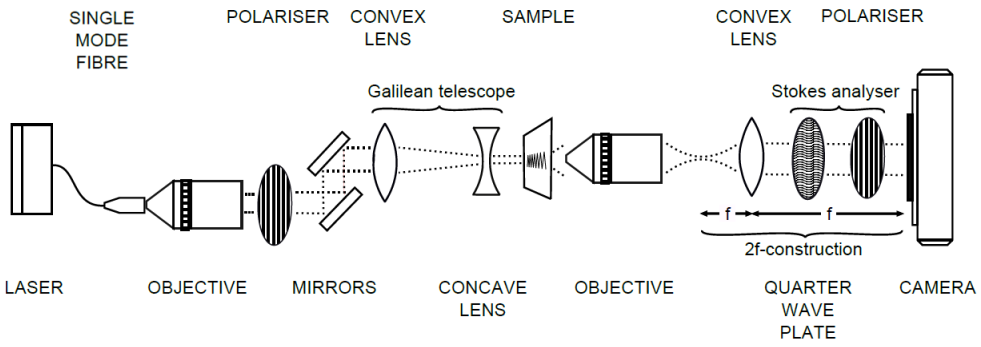


Figure 12: Schematic of the experimental setup. The polarised light from the laser, controlled by a linear polariser and narrowed by a set of lenses, illuminates the gold side of the sample. The light from the far-field of the sample is projected onto the camera by the objective and a lens in a 2f-construction. It passes through a computer-controlled quarter-wave plate and linear polariser, which separate out the components of the polarisation.

**Material**

This section describes the materials used in the experiment. In the experiment I studied the diffraction from a zigzag slit that was designed to act as a quarter-wave plate. The setup was designed to measure the polarisation of the light in the near and far field, making use of a so-called Stokes analyser. I illuminated the zigzag with 830 nm and 633 nm light. To image the zigzag clearly, some adjustments were made to the setup of the 830 nm measurements. First I shall describe the general setup and later I shall detail the specifics of this setup at 830 and 633 nm.

**General setup:** See figure 12.

The first part of the experimental setup is a laser beam. It is coupled into a single mode fibre. Via a microscope objective with NA (numerical aperture) 0.12 it couples out a Gaussian beam.

The polarisation of the laser beam is then controlled by a linear polariser (Polarcor, with a range from 740 to 860 nm. At 633 nm the approximate ratio between the transmission quotient perpendicular and parallel to the pass axis is still only 2.5:100. ).

Subsequently the ray reflects off two infrared mirrors which reflect wavelengths between 600 and 1000 nm. The light then propagates through a convergent lens and a divergent lens. These lenses form an inverted Galilean telescope that compresses the beam, so the FWHM beam size is 235 microns.

Then the beam hits the sample. The sample consists of a 200 nm thick layer of gold that is attached to a 0.5 millimetre thick borosilicate glass substrate by a 10 nm titanium adhesion layer. It is assumed that the titanium adhesion layer is too thin to affect the coupling of the light from the slit and the surface plasmons.
In the gold film zigzags have been etched by ion beam milling, using a focused $Ga^+$ beam. This was done at the National Centre for High Resolution Electron Microscopy in Delft, using a FEI dual ion beam and scanning electron microscope.
On the film there are 4 zigzags where the segments are at 90 degree angles and 4 where they are at 120 degree angles. A single zigzag consists of 20 straight cuts, which have a length of 10 microns, and a width of 200 nm (See Figure 1).

The sample is mounted on an xz-translator, which can shift it in small steps. On the xz-translator the sample is mounted so it has an additional 4 degrees of freedom, although these can only roughly reposition the sample.
The light that is transmitted through the sample is collected by a 20× microscope objective, with 0.4 NA. For the purpose of alignment this objective is attached to an xyz-translator. Using a lens in a 2f-construction the Fraunhofer diffraction pattern is projected, through a Stokes analyser, on an Apogee Alta U1 camera. The Stokes analyser is a quarter-wave plate followed by a linear polariser, which can both rotate under computer control.

By removing the 2f-lens from the setup, and adjusting the focus of the objective, this setup can also image the near field of the slit.

**830 nm:** The laser used in this setup is an 830 nm laser beam (Thorlabs LPS-830-FC), which is coupled directly into a single mode fibre. There is a quarter-wave plate in the Stokes analyser for a wavelength of 830 nm. In this setup an ND filter was attached to the camera to reduce the transmitted intensity.

**633 nm:** The laser in this setup is a 633 nm helium neon laser (JDS Uniphase 1101P). This laser is coupled into a single mode fibre using two mirrors, which are highly reflective at wavelengths between 400 and 700 nm. Due to chromatic aberration of the lens there is a shift in the focus of the Galilean telescope. To correct for the shift at this wavelength, an extra lens is added. There is a quarter-wave plate placed in the Stokes analyser that functions at a wavelength of 633 nm.

**Method**

The experiment is set up to find the spatially dependent local polarisation in the diffraction pattern. The polarisation of light is characterized by the Stokes parameters (see the definition in the Theory section). In order to determine these parameters, I employed the Stokes analyser. The Stokes analyser and the camera are connected to a computer. This computer runs two coupled programs. One program controls the rotation of the quarter wave plate and the linear polariser, the other program then tells the camera to take pictures. The Stokes analyser is oriented to transmit certain components of the intensity (see Figure 13), and pictures are taken. This set of pictures is then imported into a final program, which calculates the Stokes parameters from the intensities of the pictures.

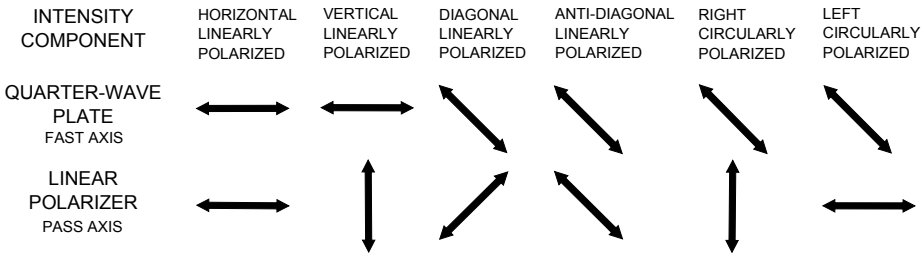


Figure 13: Orientation of the Stokes analyser for determining each intensity component needed to calculate the Stokes parameters, seen along the direction of the light.

# 4 Results

There are different results for the two different setups. These results give the polarisation from the zigzags and the polarisation and intensity of the diffraction pattern. I will make use of two ways of representing the polarisation. Firstly through the normalised Stokes parameters, which allows for comparison to the theoretical description, and secondly through polarisation ellipses. These polarisation ellipses are the envelope of the point of the electric field vector over an entire period. The direction of rotation of these ellipses is indicated by the colour. Here orange signifies right-handed rotation, blue signifies left-handed rotation and gray signifies a linear polarisation.
To create these representations I have used MATLAB.
The information is processed by reducing the noise in the images and then carrying out the division to obtain the normalised Stokes parameters.
Then I choose a lattice of points, where these ellipses will be plotted, and find their Stokes parameters. The parameters of the polarisation ellipses can be calculated from the Stokes parameters. MATLAB doesn't have a function to plot the ellipses on the lattice, so I made use of the program plot_ellipse [5].

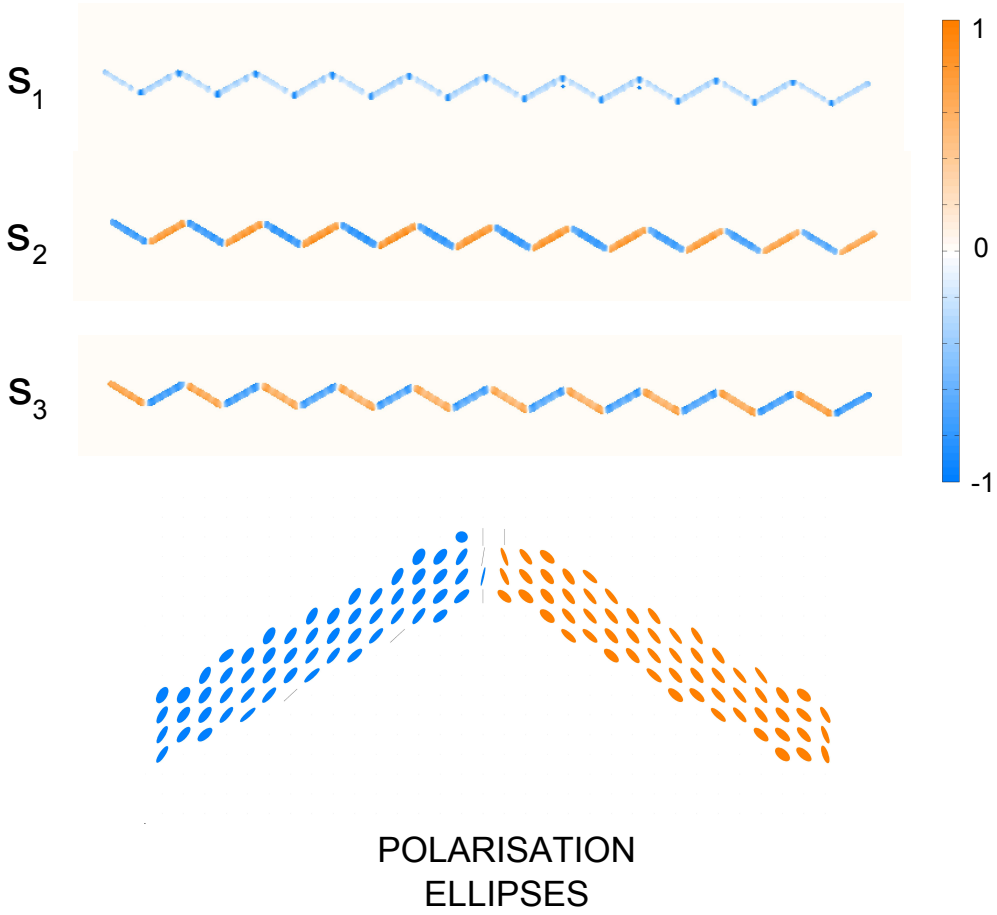


Figure 14: The polarisation of the near field of the 120° zigzag grating, illuminated by 830 nm light. If $s_1$ is positive then the polarisation has a horizontal component; if negative, then it is vertical. If $s_2$ is positive then the polarisation has a diagonal component; if negative, then it is anti-diagonal. If $s_3$ is positive then the polarisation has a right-handed component; if negative, then it is left-handed. The relative saturations indicate their contribution to the total polarisation. The color of the polarisation ellipses indicates their handedness and is defined the same as that of $s_3$.

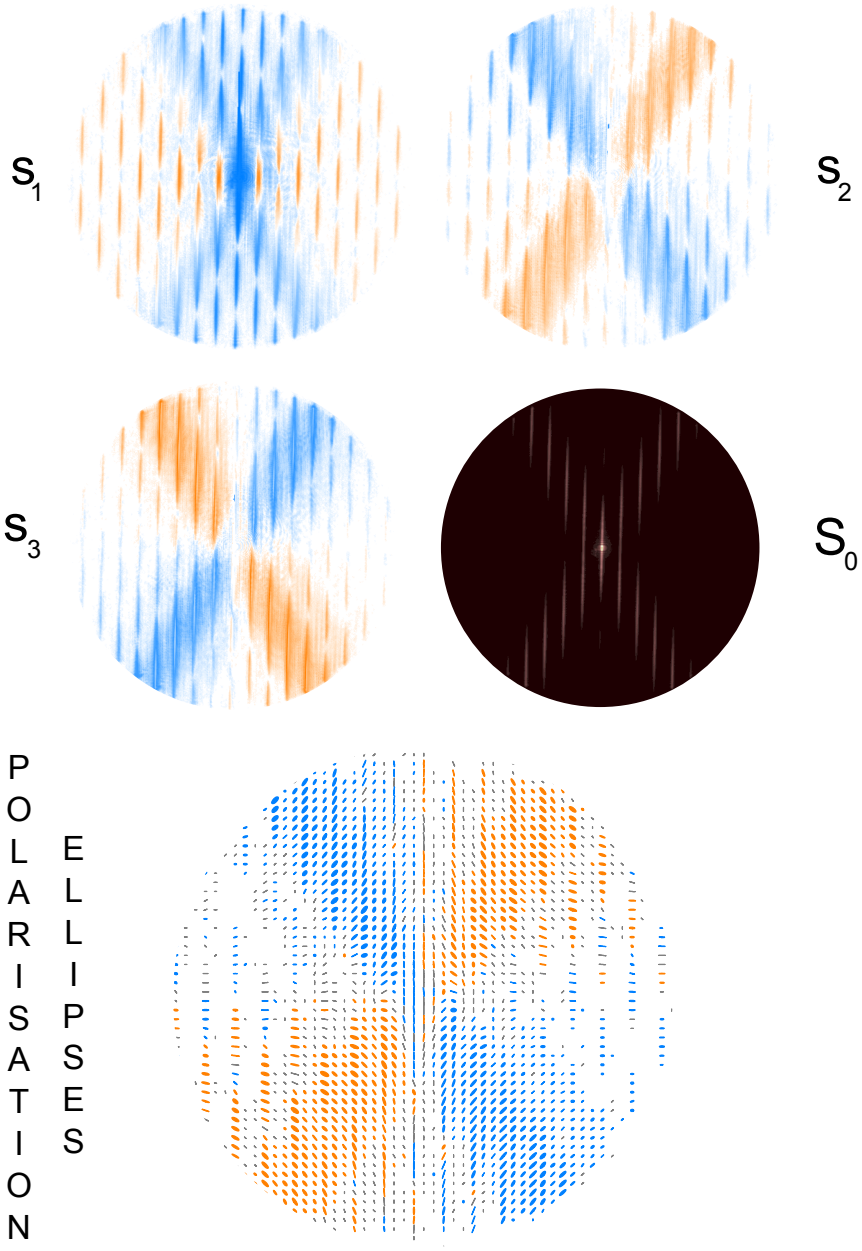


Figure 15: The polarisation of the far-field of the diffraction pattern of the 120° zigzag, illuminated by 830 nm light. If $s_1$ is positive then the polarisation has a horizontal component; if negative, then it is vertical. If $s_2$ is positive then the polarisation has a diagonal component; if negative, then it is anti-diagonal. If $s_3$ is positive then the polarisation has a right-handed component; if negative, then it is left-handed. The relative saturations indicate their contribution to the total polarisation. The color of the polarisation ellipses indicates their handedness and is defined the same as that of $s_3$.

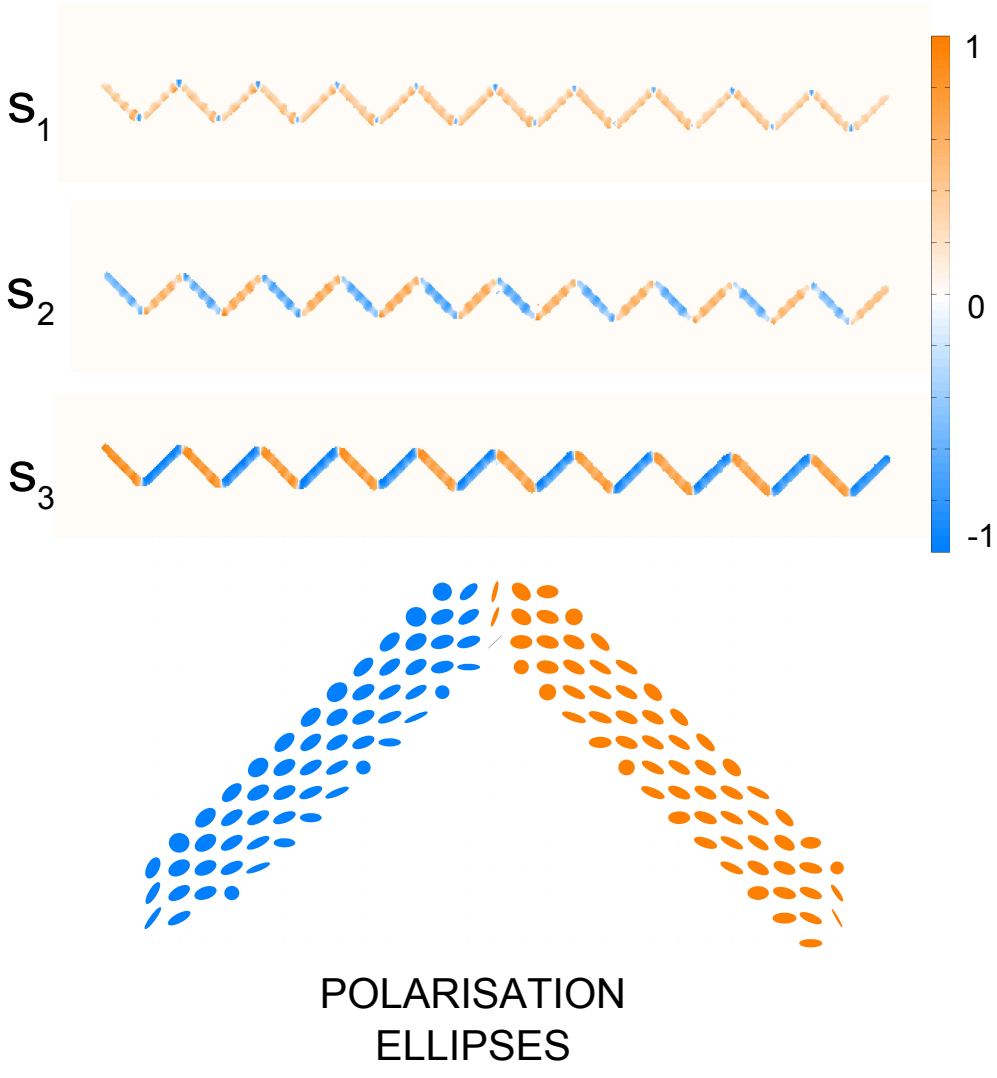


Figure 16: The polarisation of the near field of the 90° zigzag grating, illuminated by 830 nm light. If $s_1$ is positive then the polarisation has a horizontal component; if negative, then it is vertical. If $s_2$ is positive then the polarisation has a diagonal component; if negative, then it is anti-diagonal. If $s_3$ is positive then the polarisation has a right-handed component; if negative, then it is left-handed. The relative saturations indicate their contribution to the total polarisation. The color of the polarisation ellipses indicates their handedness and is defined the same as that of $s_3$.

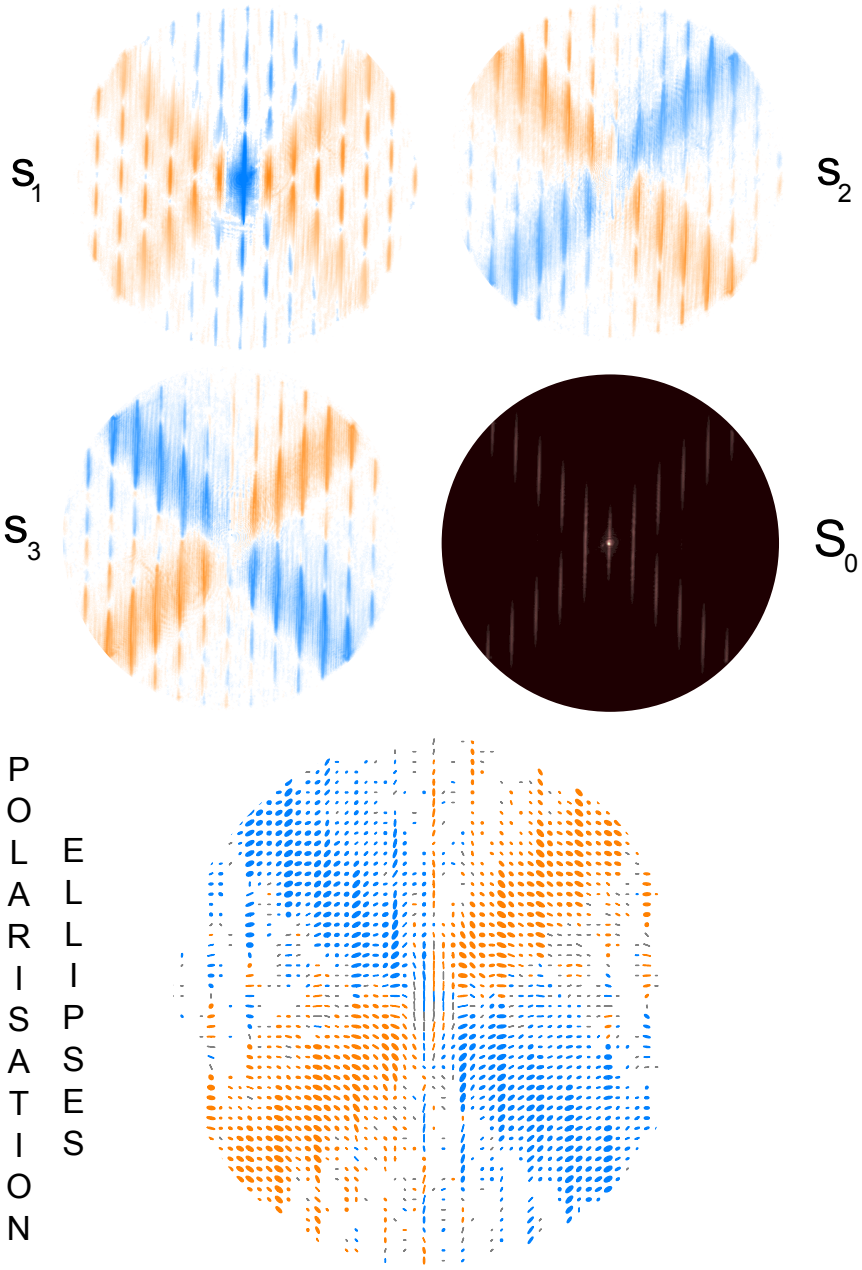


Figure 17: The polarisation of the far-field diffraction pattern of the 90° zigzag, illuminated by 830 nm light. If $s_1$ is positive then the polarisation has a horizontal component; if negative, then it is vertical. If $s_2$ is positive then the polarisation has a diagonal component; if negative, then it is anti-diagonal. If $s_3$ is positive then the polarisation has a right-handed component; if negative, then it is left-handed. The relative saturations indicate their contribution to the total polarisation. The color of the polarisation ellipses indicates their handedness and is defined the same as that of $s_3$.

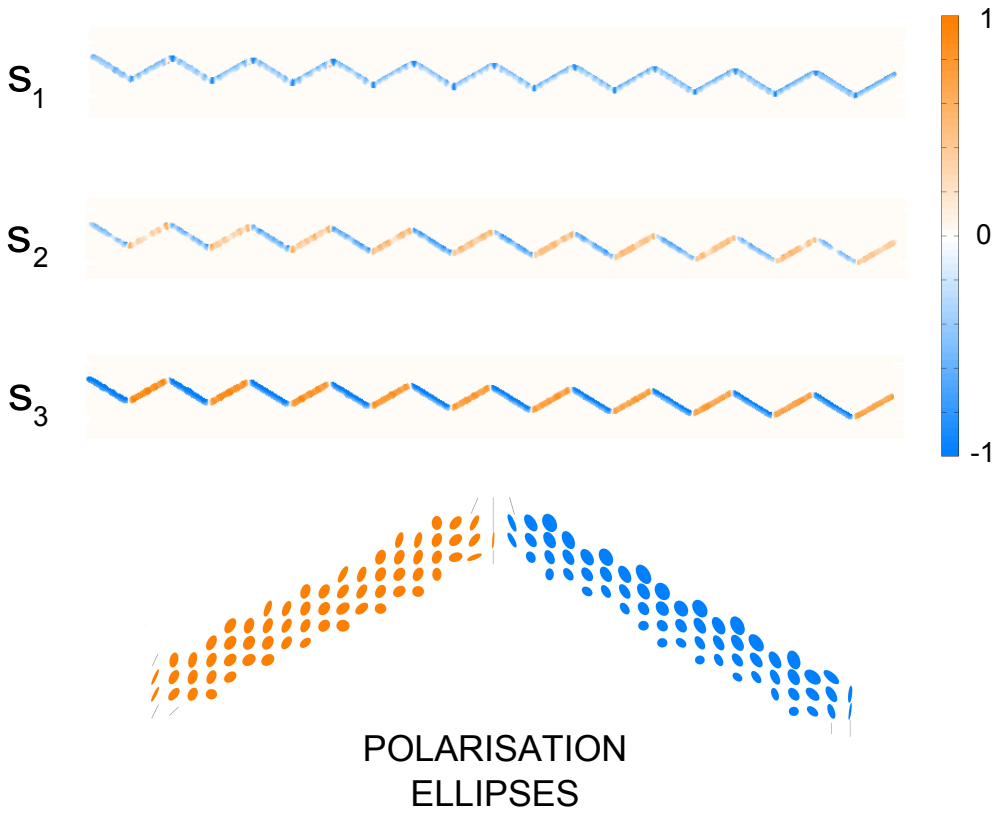


Figure 18: The polarisation of the near field of the 120° zigzag grating, illuminated by 633 nm light. If $s_1$ is positive then the polarisation has a horizontal component; if negative, then it is vertical. If $s_2$ is positive then the polarisation has a diagonal component; if negative, then it is anti-diagonal. If $s_3$ is positive then the polarisation has a right-handed component; if negative, then it is left-handed. The relative saturations indicate their contribution to the total polarisation. The color of the polarisation ellipses indicates their handedness and is defined the same as that of $s_3$.

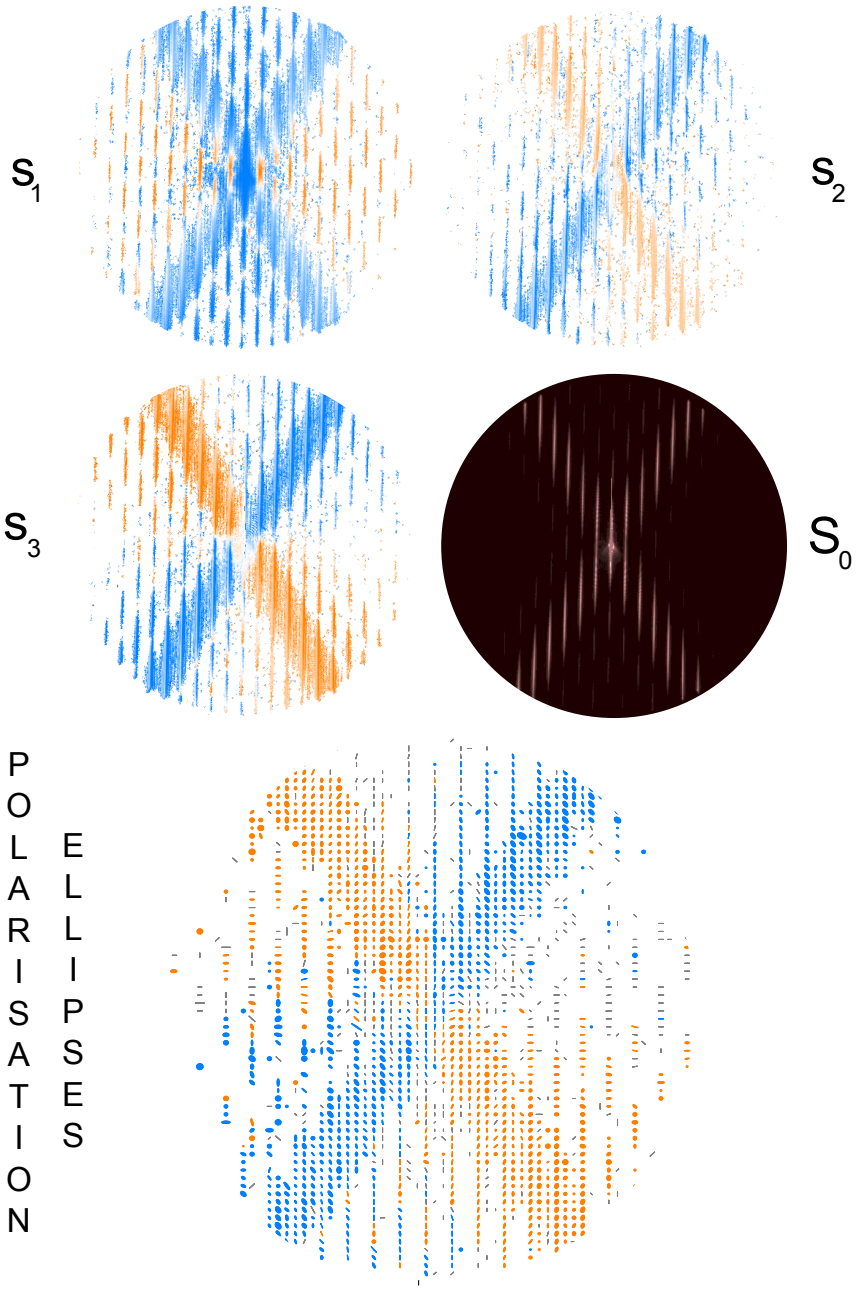


Figure 19: The polarisation of the far-field diffraction pattern of the 120° zigzag, illuminated by 633 nm light. If $s_1$ is positive then the polarisation has a horizontal component; if negative, then it is vertical. If $s_2$ is positive then the polarisation has a diagonal component; if negative, then it is anti-diagonal. If $s_3$ is positive then the polarisation has a right-handed component; if negative, then it is left-handed. The relative saturations indicate their contribution to the total polarisation. The color of the polarisation ellipses indicates their handedness and is defined the same as that of $s_3$.

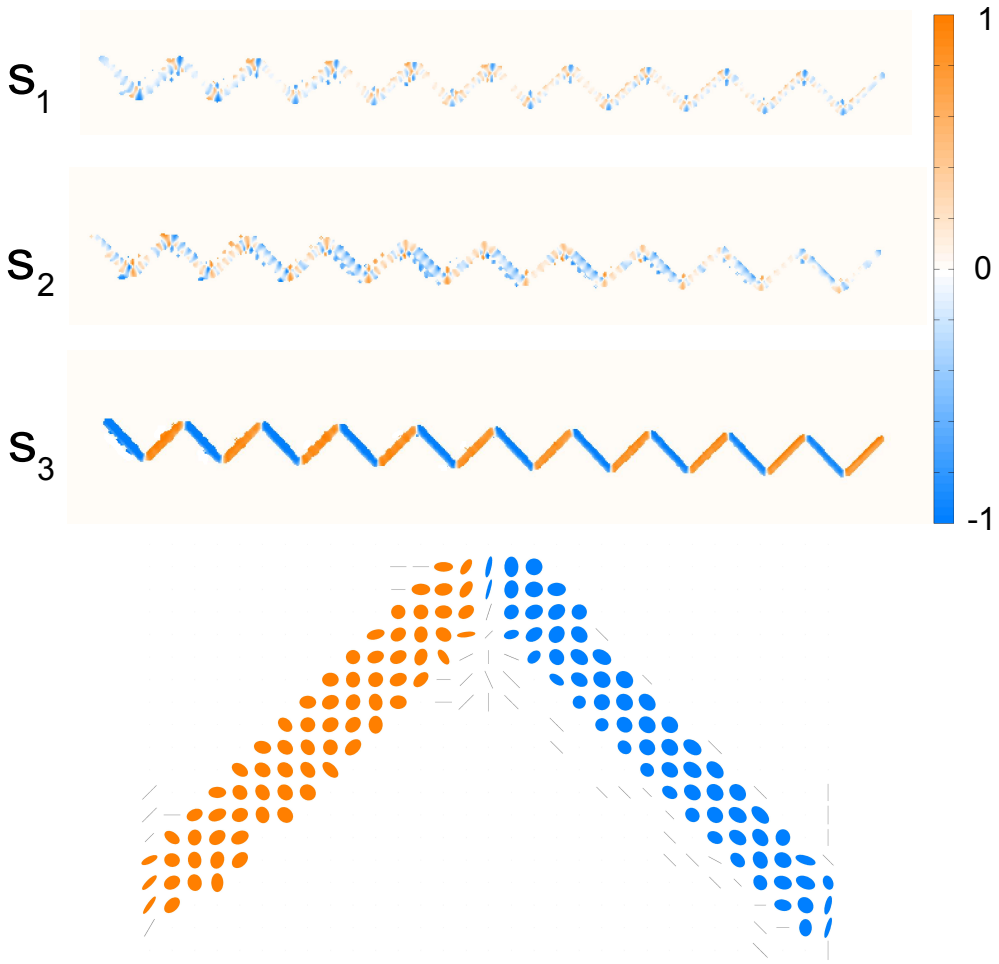


Figure 20: The polarisation of the near field of the 90° zigzag grating, illuminated by 633 nm light. If $s_1$ is positive then the polarisation has a horizontal component; if negative, then it is vertical. If $s_2$ is positive then the polarisation has a diagonal component; if negative, then it is anti-diagonal. If $s_3$ is positive then the polarisation has a right-handed component; if negative, then it is left-handed. The relative saturations indicate their contribution to the total polarisation. The color of the polarisation ellipses indicates their handedness and is defined the same as that of $s_3$.

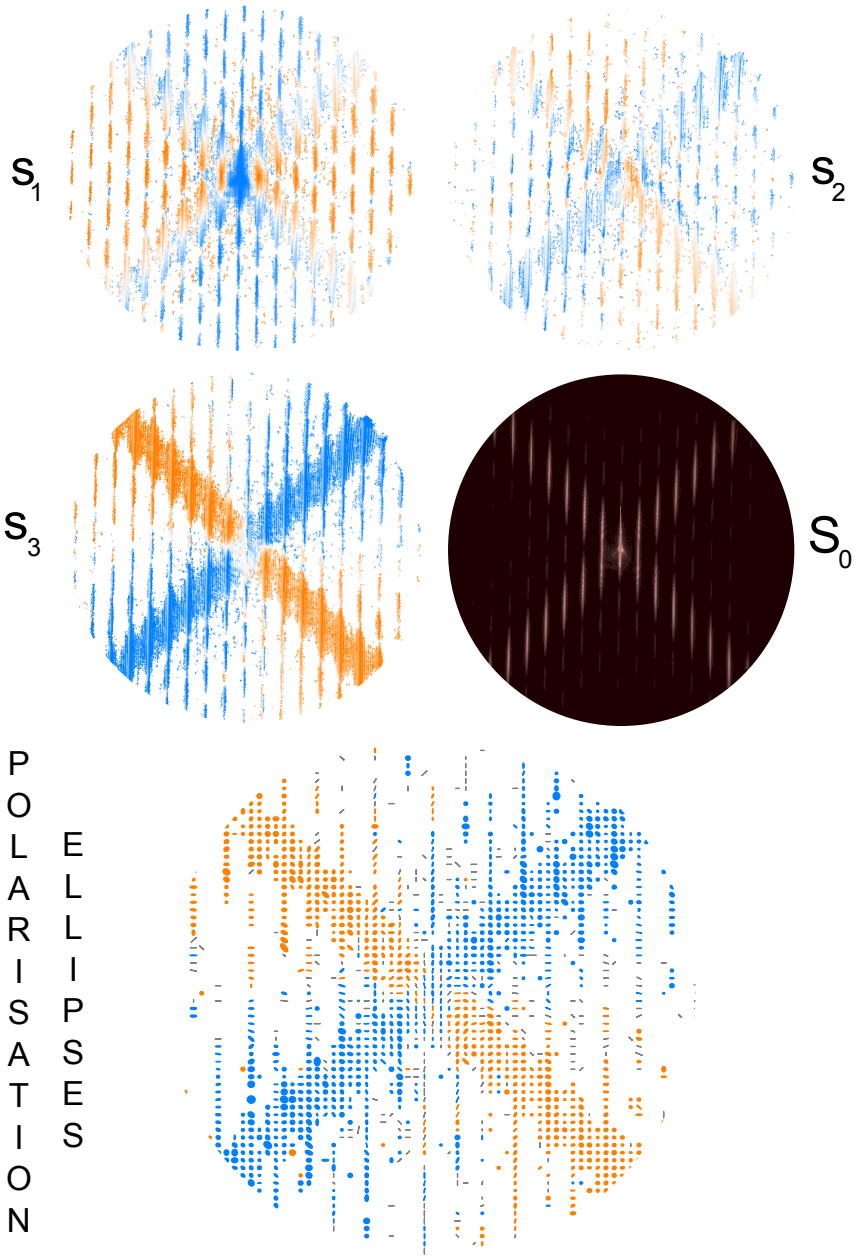


Figure 21: The polarisation of the far-field diffraction pattern of the 90° zigzag, illuminated by 633 nm light. If $s_1$ is positive then the polarisation has a horizontal component; if negative, then it is vertical. If $s_2$ is positive then the polarisation has a diagonal component; if negative, then it is anti-diagonal. If $s_3$ is positive then the polarisation has a right-handed component; if negative, then it is left-handed. The relative saturations indicate their contribution to the total polarisation. The color of the polarisation ellipses indicates their handedness and is defined the same as that of $s_3$.

# 5 Discussion

**Differences between the model and measurement**

The model and the measurements look similar, but not quite the same. This is because there are factors in the measurements that ideally shouldn't occur: According to the functional definition of the Stokes parameters (see Theory), only the intensity is an addition. As such, $S_0$ is the only parameter with an offset intensity derived from the background noise. This can be accounted for in the simulation by adding a small constant to $S_0$, which represents this contribution of the noise to the intensity, before determining the normalised Stokes parameters.

In the $s_1$ diffraction images there is a central blue spot. This spot is the result of the transmission of the laser light through the metal. This light isn't visible when looking at a focused image of the zigzags. When looking at the Fraunhofer diffraction image however, this entire background contribution adds up to a powerful $0^{th}$ order peak. This peak is visible even when the beam doesn't pass through a grating.
The peak can be modelled by the Fourier transform of a 'top-hat function', which represents the background field that falls into the objective. The result of the Fourier transform is a Bessel function.
The diffraction images have a circular shape, this is the result of a cutoff of the far field by the NA of the objective behind the sample. This can be modelled by a mask.
These adjustments have been made in Figures 22 and 23. These are very similar to the results in Figures 21 and 19. I will therefore use my interpretation from the Theory section, to comment on my results.

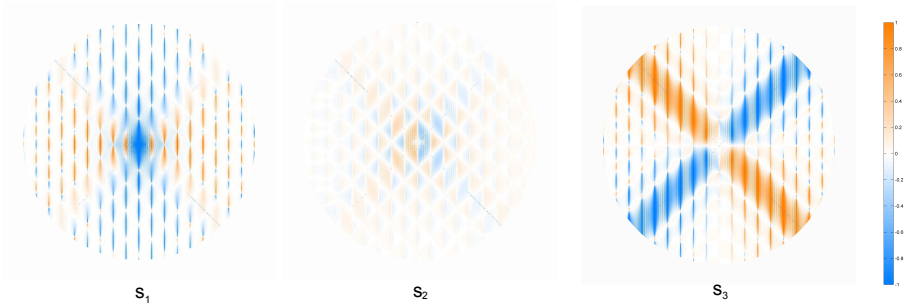


Figure 22: A simulation of the 90° zigzag diffraction pattern, adjusted for an offset background noise in $S_0$ and an additional vertical transmission, transmitted through the metal. If $s_1$ is positive then the polarisation has a horizontal component; if negative, then it is vertical. If $s_2$ is positive then the polarisation has a diagonal component; if negative, then it is anti-diagonal. If $s_3$ is positive then the polarisation has a right-handed component; if negative, then it is left-handed. The relative saturations indicate their contribution to the total polarisation.

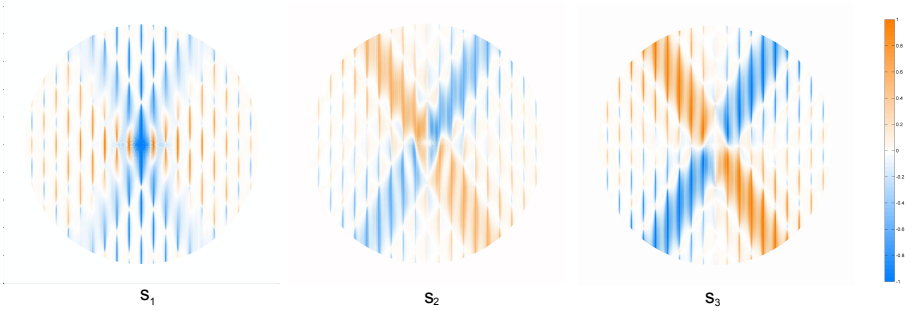


Figure 23: A simulation of the 120° zigzag diffraction pattern, adjusted for an offset background noise in $S_0$ and an additional vertical transmission, transmitted through the metal. If $s_1$ is positive then the polarisation has a horizontal component; if negative, then it is vertical. If $s_2$ is positive then the polarisation has a diagonal component; if negative, then it is anti-diagonal. If $s_3$ is positive then the polarisation has a right-handed component; if negative, then it is left-handed. The relative saturations indicate their contribution to the total polarisation.

**General discussion:**
The diffraction patterns have the greatest intensity along the directions perpendicular to the slits, in the vertical fringes that are due to the periodicity of the zigzag. The polarisation and intensity of the diagonals in the diffraction image correspond to those in the images of the slits which created those diagonals. This can be seen clearest from the polarisation ellipses images of the diffraction pattern, which show ellipses similar to those of the slit.

The diffraction patterns also have a complex structure in the quadrants between these diagonals. The pictures taken of the sample, illuminated under 830 nm light (see Figures 17 and 15), do not suffer as much from noise. The images of the polarisation ellipses show how the polarisation of the light in the quadrants is dependent on the overlap of the orders of the sinc-function: When moving from one diagonal to another, along a horizontal or vertical line, the polarisation of the light varies between the polarisations of those diagonals through a linear polarisation. This is evidenced by a rotation and flattening of the polarisation ellipses toward the centre of such a path.
An interesting feature of these superpositions of polarisation is the blue vertical fringe, in the centre of the $s_1$ diffraction pattern (see for instance $s_1$ of Figure 17). This fringe is due to the overlap of the opposite elliptical polarisations of the diagonals. Similarly, in the $s_1$ image of the slits (see Figure 16), there is an overlap of the circular polarisations in the angles, which leads to an additional vertical polarisation.

**830 nm:** It is clear from the polarisation ellipse image of the slits (Figure 16), that the slits don't behave like quarter-wave plates at this wavelength. Making use of Figure 16 one can find that the slits behave rather like $\frac{3\lambda}{8}$ plates and emit an elliptical polarisation. This means that along the diagonals of the diffraction pattern the light is also elliptically polarised and in the quadrants the polarisation is an intermediate state (see Figure 17).
In the images of the slits there appears to be an oscillation in the intensity along the length of the slits. Because I observe only four oscillations, and twelve wavelengths would fit the length, it is more likely that this is a consequence of the diffraction from the slit rather than a standing mode.

**633 nm:** The intensity on the sample was lower at this wavelength. This is evident in the amount of noise in the images. The strength of the circularly polarised component is greater and so $s_1$ and $s_2$ suffer more strongly from the noise.
In Figures 20 and 18 there also seems to be an oscillation in the intensity. Now, besides an ill-matched number of oscillations, the oscillation has different polarisations in Figure 20; this also indicates it is an artifact due to overlapping diffraction fringes.

Despite the noise, Figure 21 shows that on the diagonals $s_1$ and $s_2$ are weak. This results from the nearly circularly polarised light from the slits (see Figure 20) and, when you move away from the centre, very little mixing of the opposite circular polarisations along the diagonals. However, for those very reasons, $s_3$ has a strong colour saturation along the diagonals. This means the light is strongly circularly polarised along the diagonals of the diffraction pattern.
The noise makes it difficult to interpret the polarisation ellipses in the quadrants of Figure 21, as done previously for those at 830 nm. Nevertheless, the normalised Stokes parameters still allow a rough assesment: Centered between two diagonals $s_3$ becomes weak and $s_1$ becomes strong, this means the polarisation has a weaker circular component and a stronger linear component. Relative to $s_1$ and $s_3$, $s_2$ is somewhat weaker and doesn't have the same clear structure. According to the model the $s_2$ should be rather weaker, because the superposition of the circular polarisation along the fringes of $S_0$ should result in a horizontal or vertical linear polarisation. This does however assume a perfect symmetry, which the experiment did not achieve, and there for there is a small diagonal linearly polarised component.
Interpreting this in terms of the polarisation means that light that is, for instance, right circularly polarised at a diagonal, becomes increasingly linear towards the midpoint of the quadrant. Moving along to the next diagonal it once again becomes more circular, although it will have a left circular polarisation. This is approximately the same description of the polarisation I obtained from the polarisation ellipses for the other wavelength.

**Outlook**

The measurements could be improved by having a gold film that doesn't transmit light, so the $0^{th}$ order peak doesn't appear. Another improvement could be a more intense 633 nm laser beam on the sample, so that the signal to noise ratio becomes more favourable.

This grating can be used to create several types of polarised light from linearly polarised light. By varying the angles of the zigzag, the polarisations of the diagonals of the diffraction pattern can be controlled, and as such the polarisation states in between. The sharpness of fringes of the pattern, can be controlled by the number of slits; their periodicity can be adjusted by the distance between the slits. Varying the width of the slit, or the wavelength, influences the polarisation. The polarisation of the light then influences the shape of the diffraction pattern.
If the zigzags were placed so there was also a vertical periodicity, then the diffraction pattern would likely be a raster with differently polarised points. Due to the superposition of different polarisations it might have a slightly different diffraction pattern.

# 6 Conclusion

In summary, I have studied the far field diffraction from zigzag gratings in a 200 nm thick gold film. The zigzag gratings had internal angles of either 90 or 120 degrees, and each straight slit had a length of 10 microns, and a width of 200 nm. These zigzags were illuminated by laser light with wavelengths of 633 and 830 nm. Under a wavelength of 633 nm these slits operated as quarter-wave plates, with their fast axes parallel to the length of the slit.

It was shown that it is possible to separate the several polarisations, but not in a neat piecewise fashion. The circular polarisation and intensity of the light is strongest along the diagonals, and corresponds to the light from the slits. Between these diagonals the polarisation ellipses are intermediates between those of the two diagonals. The 830 nm measurements show that this transition is continuous, although the handedness of the circular polarisation alternates; for 633 nm measurements this is not quite clear.

For the 633 nm the simulation gives a decent prediction of this polarisation. At 830 nm the zigzag grating doesn't behave like a quarter-wave plate and rather more like an three-eighths-wave plate.

# 7 Acknowledgements

I would like thank Philip Chimento, Eric Eliel, Paul Alkemade and Wolfgang Löffler.
Philip Chimento and Eric Eliel initiated and and supervised this project. Their suggestions and advice on the project were very productive.
Paul Alkemade etched the zigzags in the gold film.
Wolfgang Löffler made the computer programs that were used to control the Stokes analyser and the computation of the Stokes parameters.

# References

[1] P. F. Chimento, N. V. Kuzmin, J. Bosman, P. F. A. Alkemade, G. W. 't Hooft, and E. R. Eliel, A sub wavelength slit as a quarter-wave retarder, Optics Express 19, 24219 (2011).

[2] A. Roberts and L. Lin, Plasmonic quarter-wave plate, Optics Letters, 37, 11, pp. 1820-1822 (2012)

[3] A. M. Nugrowati, S. F. Pereira and A. S. van de Nes, Birefringence of small apertures for shaping ultra short pulses, arXiv:1204.3478v1

[4] D . S. Kliger, J. W. Lewis, and C. E. Randall, (1990), Polarized light in optics and spectroscopy, Academic Press, San Diego

[5] F. Hermens, 2010, Simple ellipse plotting function, http://www.mathworks.com/matlabcentral/fileexchange/28996